Proceedings of the
47th IEEE Conference on Decision and Control
Cancun, Mexico, Dec. 9-11, 2008

Nonlinear Analysis of Cross-Coupled Oscillator Circuits

Xiaoqing Ge, Murat Arcak and Khaled Nabil Salama

Abstract— **We study global stability properties of a class of cross-coupled oscillators which admit the representation of a dynamic system in feedback with a static nonlinearity. We present sufficient conditions for almost global convergence of the solutions to a limit cycle when the feedback gain is in the neighborhood of the bifurcation point. The result is then extended to the synchronization of interconnected identical cross-coupled oscillators.**

I. I

Cross-coupled oscillators, which form an important class of oscillators, have been widely used in commercial applications. They are frequently employed as voltage-controlled oscillators in function generators, phase-lock loops, frequency synthesizers, etc. Some of the early stability studies were based on experimental results and linear analysis tools. Reference [1] used the Nyquist stability criterion to analyze the stability of a linearized oscillator. Reference [2] applied linear theory to the analysis of oscillation-frequency and oscillation-amplitude stability of nonlinear feedback oscillators. The key characteristics of oscillators, however, can be understood only by nonlinear analysis techniques.

In this paper we study a class of cross-coupled sinusoidal LC oscillators described by a fourth-order nonlinear model. We represent this class of cross-coupled oscillators as a Lurie system [3], which consists of a linear block in feedback with a static nonlinearity, and analyze its stability properties in the absolute stability framework.

We first prove boundedness of the trajectories using the "stiffening" property of the static nonlinearity [4]. Then we consider a general case where the linear block in the Lurie system is relative degree one and minimum phase, and the static stiffening nonlinearity is a combination of a negative slope at the origin and a static monotone increasing nonlinearity. By making the linear block passive with a Popov multiplier, we conclude following the tools in [5] that the system experiences either a supercritical pitchfork bifurcation or a supercritical Hopf bifurcation. In the case of the Hopf bifurcation we further show that a unique almost[1] globally asymptotically stable limit cycle exists.

Synchronization in systems of identical or nearly identical coupled oscillators has long been a topic of interest. Simple systems are coupled together to form a new and complex system, which maintains the dominant features of the constituents but has a more flexible behavior. Multiple, synchronized oscillator circuits are being increasingly employed in digital communications to account for the frequency drift of individual oscillators and to accommodate more than one digital standard. In this paper we consider an interconnection of identical cross-coupled oscillators through a linear, symmetric input-output coupling. By appropriately selecting the interconnection matrix and key parameters of each oscillator, we achieve an exponential synchronization of interconnected cross-coupled oscillators.

II. S M

Cross-coupled oscillators are based on the idea of activating a passive LC tank resonator through a differential negative oscillator. Reference [6] established a fourth-order nonlinear model for a classical cross-coupled sinusoidal oscillator. The modeling procedure is illustrated in Figure 1:

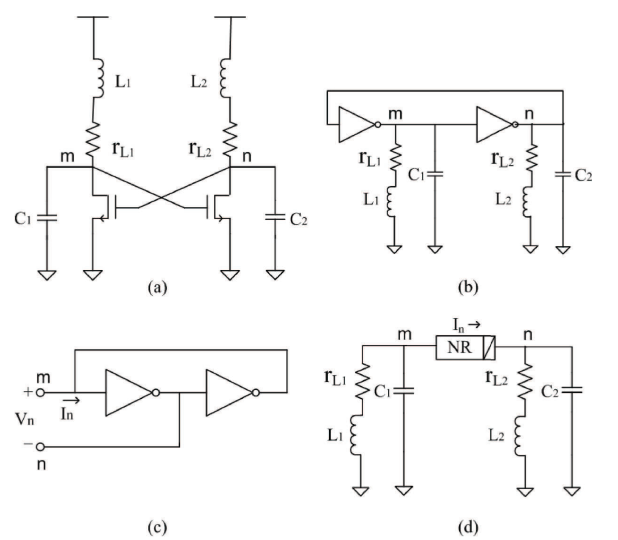

Fig. 1. Cross-coupled sinusoidal oscillator and its equivalent: (a) Cross-coupled sinusoidal oscillator. (b) Inverse-based equivalent of the oscillator. (c) Voltage-controlled nonlinear resistor consisting of two inverters. (d) Fourth-order model.

[1] By "almost" we mean convergence from all initial conditions except for those on a set of measure zero.

This work was supported by NSF under grant ECCS-0238268.

Xiaoqing Ge is with the Department of Electrical, Computer and Systems Engineering, Rensselaer Polytechnic Institute, Troy, NY 12180, USA. gex@rpi.edu

Murat Arcak is with Faculty of Electrical, Computer and Systems Engineering, Rensselaer Polytechnic Institute, Troy, NY 12180, USA. He is also with Faculty of Electrical Engineering and Computer Sciences, University of California, Berkeley, CA 94720, USA. arcakm@rpi.edu, arcak@eecs.berkeley.edu

Khaled Nabil Salama is with Faculty of Electrical, Computer and Systems Engineering, Rensselaer Polytechnic Institute, Troy, NY 12180, USA. salamk@rpi.edu

978-1-4244-3124-3/08/$25.00 ©2008 IEEE

In Figure 1(a), each transistor with its resistive load forms one common-source amplifier and two such inverting amplifiers are connected via cross-coupling techniques. Figure 1(b) shows an inverter-based equivalent of the circuit. By looking at the input characteristic between nodes m and n, we get Figure 1(c) in which two connected inverting amplifiers form a monotone cubic-type differential negative resistor characterized by [7]

$$I_n = g_0 V_n[(\frac{V_n}{V_0})^2 - 1], \tag{1}$$

where I_n is the current flowing into the resistor, V_n is the voltage across the resistor, V_0 is the zero crossing voltage and g_0 is the slope at the origin. The fourth-order nonlinear model in Figure 1(d) is described by the following equations:

$$\begin{aligned} L_1 \dot{I}_{L_1} &= V_{C_1} - r_{L_1} I_{L_1} \\ L_2 \dot{I}_{L_2} &= V_{C_2} - r_{L_2} I_{L_2} \\ C_1 \dot{V}_{C_1} &= -I_n - I_{L_1} \\ C_2 \dot{V}_{C_2} &= I_n - I_{L_2} \end{aligned} \tag{2}$$

where I_n is given by (1) with $V_n = V_{C_1} - V_{C_2}$. For a symmetric design we choose $L_1 = L_2 = L,\ C_1 = C_2 = C,\ r_{L1} = r_{L2} = r_L$.

Introducing the dimensionless variables $x(t) = V_{C_1}(t)/V_0$, $y(t) = V_{C_2}(t)/V_0$, $z(t) = r_{L_1} I_{L_1}(t)/V_0$, $w(t) = r_{L_2} I_{L_2}(t)/V_0$, $\tau = t/\sqrt{LC}$, and letting $q = \sqrt{L/C}/r_L$, $A_d = g_0 r_L$, we rewrite (2) as:

$$\begin{aligned} \begin{pmatrix} \dot{x} \\ \dot{y} \\ \dot{z} \\ \dot{w} \end{pmatrix} &= \begin{pmatrix} 0 & 0 & -q & 0 \\ 0 & 0 & 0 & -q \\ 1/q & 0 & -1/q & 0 \\ 0 & 1/q & 0 & -1/q \end{pmatrix} \begin{pmatrix} x \\ y \\ z \\ w \end{pmatrix} + \begin{pmatrix} q \\ -q \\ 0 \\ 0 \end{pmatrix} u \\ Y &= \begin{pmatrix} 1 & -1 & 0 & 0 \end{pmatrix} \begin{pmatrix} x & y & z & w \end{pmatrix}^T \end{aligned} \tag{3}$$

where the input $u = -\phi_k(Y)$ depends on the static nonlinearity

$$\phi_k(Y) = -kY + kY^3. \tag{4}$$

The parameter $k = A_d > 0$ controls the negative slope at the origin of $\phi_k(\cdot)$.

Note that the linear block (3) can be decomposed into observable and unobservable subsystems, denoted by G_O and $G_{\bar{O}}$, respectively. Using the change of variables $(\tilde{x}, \tilde{y}, \tilde{z}, \tilde{w})' = (x, z, x-y, z-w)'$, we obtain the observable subsystem G_O:

$$\begin{aligned} \begin{pmatrix} \dot{\tilde{z}} \\ \dot{\tilde{w}} \end{pmatrix} &= \begin{pmatrix} 0 & -q \\ 1/q & -1/q \end{pmatrix} \begin{pmatrix} \tilde{z} \\ \tilde{w} \end{pmatrix} + \begin{pmatrix} 2q \\ 0 \end{pmatrix} u \\ Y &= \begin{pmatrix} 1 & 0 \end{pmatrix} \begin{pmatrix} \tilde{z} & \tilde{w} \end{pmatrix} \end{aligned} \tag{5}$$

and the unobservable subsystem $G_{\bar{O}}$:

$$\begin{pmatrix} \dot{\tilde{x}} \\ \dot{\tilde{y}} \end{pmatrix} = \begin{pmatrix} 0 & -q \\ 1/q & -1/q \end{pmatrix} \begin{pmatrix} \tilde{x} \\ \tilde{y} \end{pmatrix} + \begin{pmatrix} q \\ 0 \end{pmatrix} u. \tag{6}$$

With this decomposition, we represent the feedback interconnection (3)-(4) as in Figure 2, where $G_{\bar{O}}$ is the stable linear system (6) driven by $u = -\phi_k(Y)$. This cascade structure implies that the stability properties are determined by the feedback loop of G_O and $\phi_k(\cdot)$.

The structure and, as we shall see, the behavior of (4)-(5) differs from standard negative-resistance oscillators and calls for the nonlinear analysis presented next.

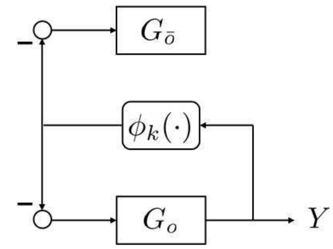

Fig. 2. Block diagram of the system (3)-(4) decomposed into its observable and unobservable components.

III. N A

A. Boundedness of Trajectories

To prove boundedness of trajectories we use the following lemma from [4], which establishes a boundedness mechanism for systems consisting of a linear block $G(s)$ in negative feedback with a static nonlinearity $\phi(\cdot)$:

***Lemma** 1:* Suppose $G(s)$ is relative degree one and minimum phase, and its high frequency gain k_p is positive. If $\phi(y)$ is stiffening, i.e. for every $m > 0$, there exists $l > 0$ such that

$$|y| \geqslant l \Rightarrow \frac{\phi(y)}{y} \geqslant m, \tag{7}$$

then the solutions of the feedback system are ultimately bounded.

In the feedback system in Figure 2, we note from (5) that

$$G_O(s) = \frac{2q(s + 1/q)}{s^2 + s/q + 1}, \tag{8}$$

which is relative degree one, minimum phase, and has a positive high frequency gain. Since $\phi_k(\cdot)$ satisfies the stiffening property, by Lemma 1, the solutions of the feedback system are ultimately bounded.

B. Hopf Bifurcation and Global Oscillations

In this part we first analyze the nonlinear dynamics of a general class of Lurie systems consisting of a linear block G and a static stiffening nonlinearity

$$\phi_k(\cdot) = -ky + \phi(\cdot), \tag{9}$$

as shown in Figure 3. Then we apply the result to the cross-coupled oscillator in a corollary. We denote by G_k the positive feedback interconnection of G and the feedback gain k. Then the feedback system of G and $\phi_k(\cdot)$ is equilvalently described as the interconnection of G_k and $\phi(\cdot)$.

The next theorem follows from a combination of Theorem 3 in [5] and Lemma 3 given in the appendix:

***Theorem** 1:* Consider the feedback system in Figure 3. Assume that the linear block G is observable with the transfer function:

$$G(s) = \frac{d(s + c)}{s^2 + as + b}, \tag{10}$$

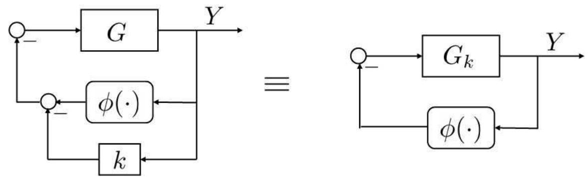

Fig. 3. Equivalent representation of the feedback interconnection of G and $\phi_k(\cdot)$.

where $a \geqslant c > 0,\ b \geqslant 0,\ d > 0,\ ac \neq b$. The nonlinearity $\phi(\cdot)$ in (9) is a smooth sector nonlinearity in $(0,+\infty)$ satisfying $\phi'(0) = \phi''(0) = 0,\ \phi'''(0) = K > 0$. Let $k^* \geqslant 0$ be the minimal value for which $G_k(s)$ has a pole on the imaginary axis and $k \gtrsim k^*$ denote a value near the bifurcation, i.e. $k \in (k^*, \bar{k}]$ for some $\bar{k} > k^*$.

Case (1): If $G_{k^*}(s)$ has a unique pole on the imaginary axis, then the bifurcation is a supercritical pitchfork bifurcation. For $k \gtrsim k^*$, the origin is a saddle node and its stable manifold $E_S(0)$ separates the whole space into two sets, each of which is the basin of attraction of a stable equilibrium.

Case (2): If $G_{k^*}(s)$ has a unique pair of conjugated poles on the imaginary axis, then the bifurcation is a supercritical Hopf bifurcation. For $k \gtrsim k^*$, the origin is unstable and the system has a unique limit cycle which is globally asymptotically stable in $\mathbb{R}^2 \backslash \{0\}$.

Proof: First consider $a \geqslant c > 0$. It follows from Lemma 3 that $G(s)$ is positive real so the linear block is passive. Because $G(s)$ is relative degree one, minimum phase and has a positive high frequency gain, by Lemma 1, the trajectories of the feedback system of G and $\phi_k(\cdot)$ are ultimately bounded. The closed-loop transfer function of the positive feedback interconnection of G and k is:

$$G_k(s) = \frac{G(s)}{1-kG(s)} = \frac{d(s+c)}{s^2+(a-kd)s+(b-kcd)}, \tag{11}$$

so

$$k^* = \min\left(\frac{a}{d}, \frac{b}{cd}\right). \tag{12}$$

If $ac > b$, then $k^* = \dfrac{b}{cd}$,

$$G_{k^*}(s) = \frac{d(s+c)}{s^2+(a-b/c)s}, \tag{13}$$

which has a unique pole on the imaginary axis. By Lemma 3, $G_{k^*}(s)$ is either positive real or could be made positive real by adding a zero at some $\alpha > 0$. Hence, an application of Theorem in [5] shows that the bifurcation is a supercritical pitchfork bifurcation and that all solutions, except for those starting on $E_S(0)$, converge to one of the two stable equilibria.

If $ac < b$, then $k^* = \dfrac{a}{d}$,

$$G_{k^*}(s) = \frac{d(s+c)}{s^2+(b-ac)}, \tag{14}$$

which has a unique pair of conjugate poles on the imaginary axis. By Lemma 3 and Theorem 3 in [5], $G_{k^*}(s)$ can be made positive real by adding a positive zero. Thus, the bifurcation is a supercritical Hopf bifurcation and a unique limit cycle that is almost globally asymptotically stable exists. ∎

Now we use Theorem 1 to analyze the feedback loop of G_O and $\phi_k(\cdot)$.

***Corollary** 1:* Consider the feedback system (4)-(5) represented as in Figure 2. When $q > 1$, a supercritical Hopf bifurcation occurs at $k^* = \frac{1}{2q^2}$. For $k \gtrsim k^*$, the system possesses a unique limit cycle which is globally asymptotically stable in $\mathbb{R}^2 \backslash \{0\}$.

Proof: The closed loop transfer function of G_O and k is

$$G_k(s) = \frac{G_O(s)}{1-kG_O(s)} = \frac{2q(s+1/q)}{s^2+(1/q-2kq)s+(1-2k)}. \tag{15}$$

Because $q > 1$, $k^* = 1/(2q^2)$. At the bifurcation point,

$$G_{k^*}(s) = \frac{2q(s+1/q)}{s^2+(1-1/q^2)}, \tag{16}$$

which has a unique pair of conjugated poles on the imaginary axis. By Case (2) in Theorem 1, the bifurcation is a supercritical Hopf bifurcation and there exists a unique limit cycle that is globally asymptotically stable in $\mathbb{R}^2 \backslash \{0\}$ for $k \gtrsim k^*$. ∎

As stated at the end of Section II, the unobservable subsystem $G_{\bar{O}}$ is a stable system driven by $u = -\phi_k(Y)$. When the supercritical Hopf bifurcation occurs, G_O has a global asymptotically stable limit cycle in $\mathbb{R}^2 \backslash \{0\}$ and the trajectories of $G_{\bar{O}}$ remains bounded. Consequently, the cross-coupled oscillator exhibits a global oscillation.

C. Analysis for a Wider Range of Parameters and Simulations

The case we discussed above, where $q > 1$ and $k \gtrsim k^* = \frac{1}{2q^2}$, is the range of practical interest. For completeness we further investigate the nonlinear behavior of the feedback system as the parameters k and q vary in a wider range.

The equilibrium points of the system are determined by the equation:

$$q\tilde{z}(2k-1-2k\tilde{z}^2) = 0, \tag{17}$$

where $k, q > 0$. First assume that $q > 1$. When $k \leqslant \frac{1}{2}$, there is only one equilibrium point at the origin: $e_1 = (0,0)^T$. Evaluating the Jacobian matrix at e_1, we get

$$A_1 = \begin{pmatrix} 2kq & -q \\ 1/q & -1/q \end{pmatrix} \tag{18}$$

for which the real parts of the eigenvalues are $2kq^2 - 1$. When $0 < k < \frac{1}{2q^2}$, the origin is a stable focus. It follows from Popov criterion and Lemma 3 in the appendix that the system is globally asymptotically stable. As k increases, a bifurcation occurs at $k^* = \frac{1}{2q^2}$. When $\frac{1}{2q^2} < k < \frac{1}{2}$, the origin is either an unstable node or an unstable focus. Because the trajectories are bounded it follows from the Poincaré-Bendixson Theorem that there must be a limit cycle encircling the origin. When $k > \frac{1}{2}$, the eigenvalues of A_1 have opposite signs, so e_1 becomes a saddle point. Meanwhile, two new equilibrium points arise: $e_{2,3} = (\pm\sqrt{1-1/2k}, \pm\sqrt{1-1/2k})^T$, which have the same Jacobian matrices:

$$A_2 = A_3 = \begin{pmatrix} 3q-4kq & -q \\ 1/q & -1/q \end{pmatrix}. \tag{19}$$

The real parts of the eigenvalues are $\frac{1}{2q}(-4kq^2+3q^2-1)$. Thus, e_2 and e_3 are unstable nodes or foci when $\frac{1}{2} < k \leqslant \frac{3q^2-1}{4q^2}$ and become stable when $k > \frac{3q^2-1}{4q^2}$. Note that when $q \gg 1$, the system is time-scale separated, where $\tilde{z}$ settles down much more quickly than $\tilde{w}$. All the trajectories starting in the unstable manifold of the origin approach to the nullcline $\dot{\tilde{z}} = 0$. Since e_2 and e_3 are stable, the trajectories will settle down at either e_2 or e_3 after hitting the nullcline. Thus, the system is globally bistable in $\mathbb{R}^2 \backslash E_S(0)$.

Next we turn to the case $q < 1$. When $0 < k \leqslant \frac{1}{2}$, there is only one equilibrium point at the origin. Since $\frac{1}{2} < \frac{1}{2q^2}$, the eigenvalues of A_1 always have negative real parts. Thus, the equilibrium point e_1 is a stable node or focus. As discussed above, the system is globally asymptotically stable. When $k > \frac{1}{2}$, e_1 becomes a saddle point and two new equilibrium points e_2 and e_3 emerge. It follows from (15) that $k^* = \frac{1}{2} < \frac{1}{2q^2}$ and

$$G_{k^*}(s) = \frac{2q(s+1/q)}{s^2+(1/q-2kq)s}, \tag{20}$$

which has a unique pole on the imaginary axis. By Case (1) in Theorem 1, the bifurcation is a supercritical pitchfork bifurcation, and for $k \gtrsim k^* = \frac{1}{2}$, the system is globally bistable in $\mathbb{R}^2 \backslash E_S(0)$.

We simulate the cross-coupled oscillator in LTspice. We first select $q = 2$. When $k = 0.1$, e_1 is a globally asymptotically stable focus, as shown in Figure 4(a). Figure 4(c) shows that when k is slightly larger than $k^* = 0.125$, a limit cycle which is almost globally asymptotically stable arises. As k keeps increasing, e_1 turns into a saddle point and two unstable equilibria e_2 and e_3 emerge. All the equilibria are encircled by a limit cycle, as shown in 4(d). When $k = 1.2$, the limit cycle disappears. Trajectories starting in the unstable manifold of e_1 settle down at either e_2 or e_3.

Then we choose $q = 0.5$. When $k = 0.3$, the system has only one equilibrium e_1, which is globally asymptotically stable, as shown in Figure 5(a). When $k = 3$, e_1 becomes a saddle point and two new stable equilibria e_2 and e_3 emerge. Almost global bistability is shown in Figure 5(b). In Table I we summarize the nonlinear behavior of the feedback system for varying values of k and q.

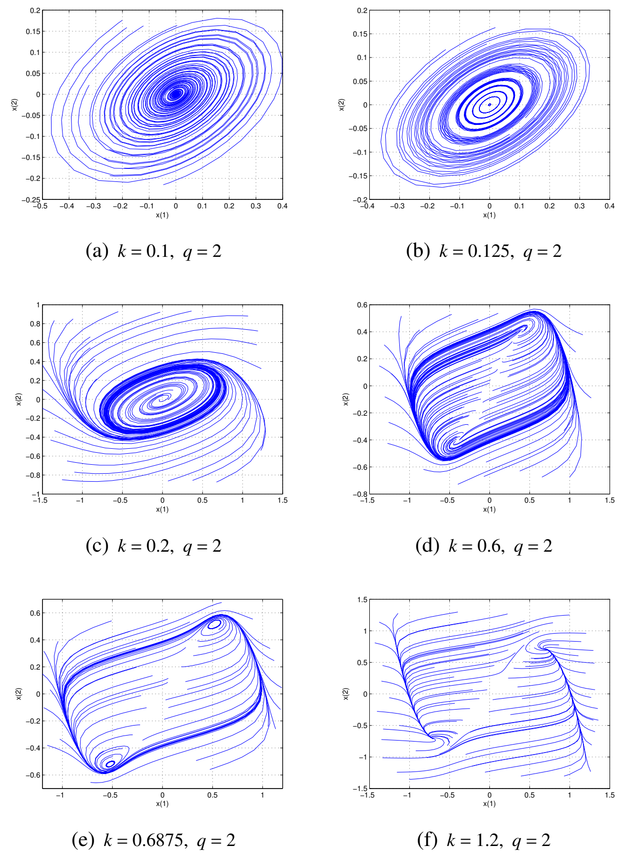

(a) $k = 0.1$, $q = 2$ (b) $k = 0.125$, $q = 2$ (c) $k = 0.2$, $q = 2$ (d) $k = 0.6$, $q = 2$ (e) $k = 0.6875$, $q = 2$ (f) $k = 1.2$, $q = 2$

Fig. 4. Phase portraits when $q > 1$

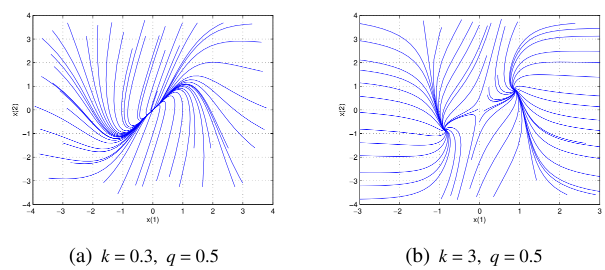

(a) $k = 0.3$, $q = 0.5$ (b) $k = 3$, $q = 0.5$

Fig. 5. Phase portraits when $q < 1$

IV. S C - O C

A. Synchronization Mechanism

Consider an interconnection of N identical, SISO oscillators, each of which is characterized by

$$\begin{cases} \dot{x}_i = Ax_i - B\phi_k(y_i) + Bu_i, & x_i \in \mathbb{R}^p \\ y_i = Cx_i, \end{cases} \tag{21}$$

where u_i and y_i are the external input and output of oscillator i, respectively. Let $U = (u_1, \ldots, u_N)^T$ be the input vector and $Y = (y_1, \ldots, y_N)^T$ be the output vector, then $U = -\Gamma Y$ indicates a linear input-output coupling through Γ. Let Γ_s denote the symmetric part of Γ and $\lambda_2(\Gamma_s)$ denote the second smallest eigenvalue of Γ_s. Let $G_k(s)$ be the positive feedback interconnection of $G(s)$ and k, where $G(s) = C(sI-A)^{-1}B$ is the transfer function of each oscillator. We denote by $k^*_{passive}$ the critical value of k above which G_k loses passivity.

***Lemma** 2:* [8] Consider the interconnection described above. Assume that (A, C) is observable, $\phi(\cdot)$ is monotone increasing and each isolated oscillator ($u_i \equiv 0$) possesses a globally asymptotically stable limit cycle in $\mathbb{R}^p \backslash E_s(0)$. If the interconnection matrix Γ is a real, positive semidefinite matrix of rank $N-1$ such that $\Gamma\mathbf{1} = \Gamma^T\mathbf{1} = 0$, where $\mathbf{1}$ denotes the column vector $(1, \ldots, 1)^T$, then for $\lambda_2(\Gamma_s) > k - k^*_{passive} > 0$, the interconnection has a limit cycle which attracts all solutions except those belonging to the stable manifold of the

TABLE I

N G_O $\phi_k(\cdot)$

	$k < \frac{1}{2}$	
$q < 1$	e_1: stable node or focus, system: globally asymptotically stable.	
	$k > \frac{1}{2}$	
$q < 1$	e_1: saddle point, e_2 and e_3 emerge: stable nodes or foci, system: globally bistable in $\mathbb{R}^2 \backslash E_S(0)$.	
	$k < \frac{1}{2q^2}$	$\frac{1}{2q^2} < k < \frac{1}{2}$
$q > 1$	e_1: stable focus, system: globally asymptotically stable.	e_1: unstable node or focus, system: unique limit cycle that is globally asymptotically stable in $\mathbb{R}^2 \backslash \{0\}$.
	$\frac{1}{2} < k < \frac{3q^2-1}{4q^2}$	$k > \frac{3q^2-1}{4q^2}$
$q > 1$	e_1: saddle point, e_2 and e_3 emerge:unstable nodes or foci, system: unique limit cycle that is globally asymptotically stable in $\mathbb{R}^2 \backslash E_S(0)$.	e_1: saddle point, e_2 and e_3: stable nodes, system: globally bistable in $\mathbb{R}^2 \backslash E_S(0)$.

origin, and all the oscillations of the network exponentially synchronize.

B. Simulations for Synchronization of Interconnected Cross-coupled Oscillators

We apply Lemma 2 to the synchronization of two interconnected identical cross-coupled oscillators described by (3) and (4). The oscillator in Figure 1(a) is designed to oscillate at 20Mhz with $L = 1\mu H$, $C = 64pF$ and $r_L = 25\Omega$. These parameters lead to $q = 5$, which implies that the condition to start oscillation is $k = 25g_0 > \frac{1}{2q^2} = 0.02$, i.e. $g_0 > 0.8mA/V$ [6].

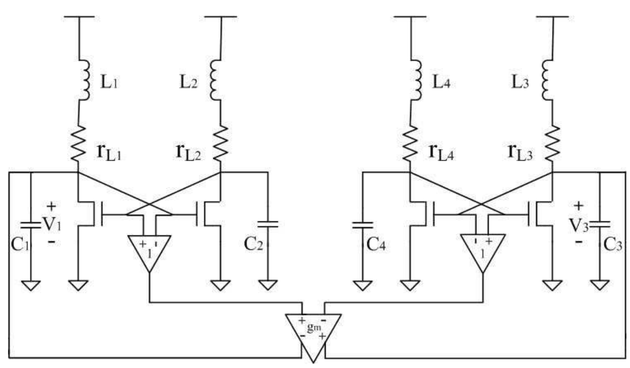

Fig. 6. Interconnection of two identical cross-coupled oscillators

From former analysis, when $q = 5$, $k = 0.025$, the oscillator possesses a globally asymptotically stable limit cycle in $\mathbb{R}^2 \backslash \{0\}$ when the external input is zero. We choose the interconnection matrix $\Gamma_1 = \begin{pmatrix} 1 & -1 \\ -1 & 1 \end{pmatrix}$, which is rank 1 and has two eigenvalues $\lambda_1(\Gamma_1) = 0$ and $\lambda_2(\Gamma_1) = 2$. For $G_O(s)$ in (8), $k^*_{passive}$=0. By Lemma 2, for $0 < k < 2$, the interconnection has a limit cycle which is globally asymptotically stable in $\mathbb{R}^2 \backslash \{0\}$, and all the oscillations exponentially synchronize. In Figure 6, two identical cross-coupled oscillators are interconnected through the matrix Γ_1. Simulation of output

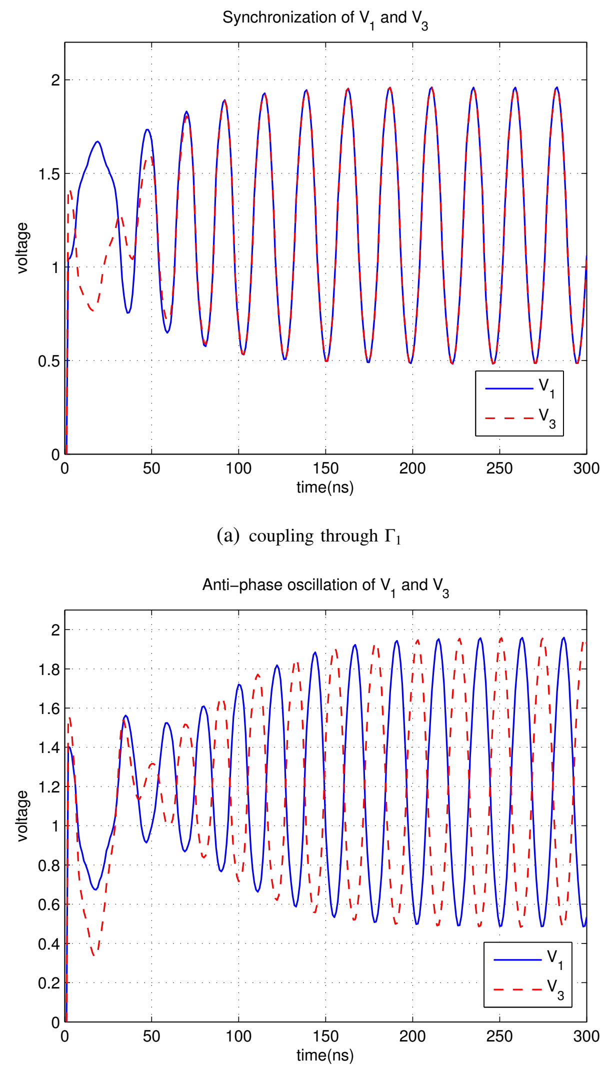

(a) coupling through Γ_1

(b) coupling through Γ_2

Fig. 7. Synchronization of two identical oscillators through linear, symmetric input-output couplings

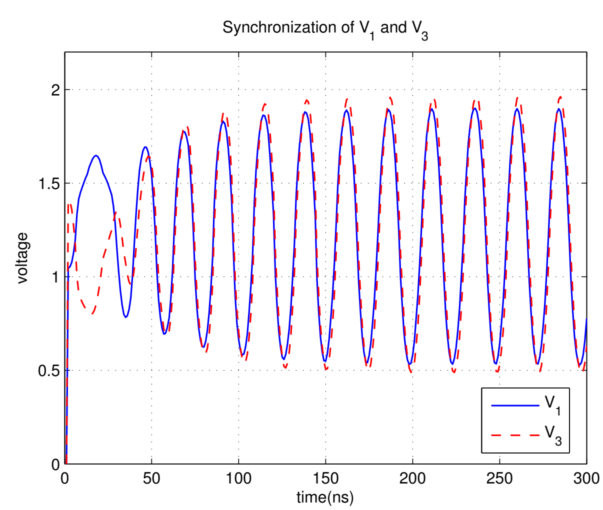

Fig. 8. Synchronization of two unmatched cross-coupled oscillators

voltages at C_1 and C_3 illustrated in Figure 7(a) exhibits a synchrone oscillation. Choosing $\Gamma_2 = \begin{pmatrix} 1 & 1 \\ 1 & 1 \end{pmatrix}$ yields an anti-phase oscillation, as shown in Figure 7(b).

The results above assume that the oscillators are identical. In real circuits, different processing methods, inductive coupling and layout mismatch can cause parameter mismatches between the oscillators, which should be taken into account in the design of synchronization scheme. Here we change the capacitances, inductances and resistances of the second oscillator by $5\% - 10\%$ of their original values. The corresponding mismatches in amplitude and phase, as shown in Figure 8, are both within 6%.

Other synchronization schemes can also be used. For example, reference [9] developed a mismatch compensation circuit to alleviate phase errors in LC quadrature voltage-controlled oscillators with a common-mode model. The synchronization frequency and amplitude will be different from those of each oscillator in this case, where one oscillator becomes a master and the others become slaves.

V. C

In this paper, we have pursued a nonlinear analysis for a particular class of cross-coupled oscillators and a synchronization scheme for the interconnection of such identical oscillators. We first presented conditions for the occurence of supercritical pitchfork or Hopf bifurcations. We then discussed the nonlinear properties as the parameters vary in a larger range. We finally discussed the synchronization of interconnected identical cross-coupled oscillators. The robustness of this synchronization scheme for interconnections of non identical oscillators is an important issue that deserves further research.

A

***Lemma** 3:* Consider the transfer function:

$$G(s) = \frac{s+c}{s^2+as+b}, \tag{22}$$

where $a, b \geqslant 0,\ a+b \neq 0,\ c > 0$. If $a \geqslant c$, then $G(s)$ is positive real. If $a < c$, then there exists a positive constant α such that $\tilde{G}(s) = (s+\alpha)G(s)$ is positive real.

Proof: A transfer function $G(s)$ is positive real [10] if:

1) All the poles of $G(s)$ have nonpositive real parts. For the poles on the imaginary axis, they should be simple with nonnegative residue;
2) The real part of $G(j\omega)$ is nonnegative.

First consider the case $a \geqslant c$. If $a^2 \leqslant 4b$, then $G(s)$ has two conjugate complex poles at $(-a \pm j\sqrt{4b-a^2})/2$, with negative real parts $-a/2$. When $a = 0$, the two poles $\pm j\sqrt{b}$ are on the imaginary axis, with the residue of $G(s)$ equal to 1. If $a^2 > 4b$, then $G(s)$ has two real poles at $(-a \pm \sqrt{a^2-4b})/2$. When $b = 0$, $G(s)$ has only one pole on the imaginary axis, with the residue $c/a > 0$. When b is nonzero, $G(s)$ has two poles in the left half-plane. It follows from (22) that

$$G(j\omega) = \frac{c + j\omega}{b - \omega^2 + ja\omega} = \frac{(a-c)\omega^2 + bc + j\omega(b-a-\omega^2)}{(b-\omega^2)^2 + a^2\omega^2}, \tag{23}$$

so the real part of $G(j\omega)$ is

$$Re\{G(j\omega)\} = \frac{(a-c)\omega^2 + bc}{(b-\omega^2)^2 + a^2\omega^2}, \tag{24}$$

which is nonnegative if $a \geqslant c$. Therefore, when $a \geqslant c$, $G(s)$ is positive real.

Next we turn to the case $a < c$. Let

$$\tilde{G}(s) = (s+\alpha)G(s) = \frac{(s+c)(s+\alpha)}{s^2+as+b}. \tag{25}$$

If $a^2 \leqslant 4b$, then $\tilde{G}(s)$ has two conjugate complex poles at $(-a \pm j\sqrt{4b-a^2})/2$, with negative real parts $-a/2$. When $a = 0$, the two poles $\pm j\sqrt{b}$ are on the imaginary axis, with the residue of $\tilde{G}(s) = c+\alpha > 0$. If $a^2 > 4b$, then $G(s)$ has two real poles at $(-a \pm \sqrt{a^2-4b})/2$, which are either in the left half-plane or merge into one pole on the imaginary axis, with the residue $c/a > 0$. Since

$$Re\{\tilde{G}(j\omega)\} \quad = \quad \frac{\omega^4 + (a\alpha + ac - c\alpha - b)\omega^2 + bc\alpha}{(b-\omega^2)^2 + a^2\omega^2}, \tag{26}$$

the sign of the real part of $\tilde{G}(j\omega)$ is determined by the polynomial $p(\omega) := \omega^4 + (a\alpha - c\alpha + ac - b)\omega^2 + bc\alpha$. To make it nonnegative, we choose α such that the roots of the equation

$$\omega^4 + (a\alpha - c\alpha + ac - b)\omega^2 + bc\alpha = 0 \tag{27}$$

are complex, that is,

$$(a\alpha - c\alpha + ac - b)^2 \leqslant 4bc\alpha. \tag{28}$$

Let $k_1 = a(c^2+b-ac)/(a-c)^2$, $k_2 = bc/(a-c)^2$, then for

$$k_1 + k_2 - 2\sqrt{k_1k_2} \leqslant \alpha \leqslant k_1 + k_2 + 2\sqrt{k_1k_2},$$

$p(\omega)$ is nonnegative and, thus, $\tilde{G}(s)$ is positive real. Note that $a < c$, so $k_1k_2 > 0$ and $k_1 + k_2 > 2\sqrt{k_1k_2}$, which ensures the positiveness of α. ■

R

[1] M. Odyniec, "Oscillator stability analysis", *Microwave Journal*, 1999.

[2] A. Borys, "Elementary deterministic theories of frequency and amplitude stability in feedback oscillators", *IEEE Transactions on Circuits and Systems*, vol. 34, pp. 254-258, 1987.

[3] A. I. Lurie and V. N. Postnikov, "On the theory of stability of control systems", *Applied Mathematics and Mechanics*, 8(3), 1944.

[4] M. Arcak, M. Larsen and P. Kokotović, "Boundedness without absolute stability in systems with stiffening nonlinearities", *European Journal of Control*, 2001.

[5] R. Sepulchre and G. B. Stan, "Feedback mechanisms for global oscillations in Lure systems", *Systems and Control Letters*, vol. 54, no. 8, pp. 809-818, 2005.

[6] A.S. Elwakil and K.N. Salama, "Improvement to the condition for oscillation of cross-coupled sinusoidal oscillators", *International Symposium on Nonlinear Theory and its Applications*, pp. 7-10, 2007.

[7] K. O'Donoghue, M. P. Kennedy and P. Forbes, "A fast and simple implementation of Chua's oscillator using a "cubic-like" Chua diode," *Proc. European Conference on Circuits Theory and Design ECCTD'05*, vol. 2, pp. 83-86, 2005.

[8] G. B. Stan and R. Sepulchre, "Analysis of interconnected oscillators by dissipativity theory", *IEEE Transactions on Automatic Control*, vol. 52, no. 2, pp. 256-270, 2007.

[9] H-J. Lee, C-S. Chen, W-S. Wuen and K-A. Wen, "A mismatch compensation circuit for CMOS quadrature VCO phase error", *International Symposium on Signals, Systems and Electronics*, pp. 497-500,2007.

[10] H. K. Khalil, *Nonlinear Systems*, Prentice Hall, 2nd edition, 1996.